Special Issue on "Theoretical and Computational Chemistry"

J. Indian Chem. Soc.,
Vol. 96, July 2019, pp. 875-882

Free energy calculations of alanine tripeptide in explicit water using temperature accelerated sliced sampling

Anji Babu Kapakayala, Abhinav Gupta, Shivani Verma and Nisanth N. Nair

Department of Chemistry, Indian Institute of Technology Kanpur, Kanpur-208 016, Uttar Pradesh, India

E-mail: nnair@iitk.ac.in

Manuscript received online 02 May 2019, revised and accepted 19 May 2019

Enhanced sampling of high dimensional free energy surfaces through molecular dynamics (MD) methods is crucial for its application in studying complex chemical reactions and conformational changes in condensed matter. Recently, we have introduced a technique called Temperature Accelerated Sliced Sampling (TASS) (*J. Chem. Phys.*, 2017, **146**, 94108) for computing high dimensional free energy surfaces in a computationally efficient manner. In this article, we demonstrate the application of this method in calculating free energy surface as a function of Ramachandran angles of alanine tripeptide in explicit water. We show that the method out-performs other conventional sampling methods like metadynamics and temperature accelerated molecular dynamics/driven-adiabatic free energy dynamics. Further, we discuss the differences between free energy surfaces *in vacuo* and in solution, and characterize different conformational states. The results of this work is of great importance as alanine tripeptide in solution is an ideal benchmark system for the methods to sample high dimensional free energy landscapes.

Keywords: Free energy calculations, enhanced sampling methods, alanine tripeptide, temperature-accelerated sliced sampling, molecular dynamics.

1. Introduction

Computational modelling of chemical reactions has become inevitable to obtain molecular level details of reaction mechanism and kinetics. Computational tools permit us to not only understand the chemical reactions taking place in an experimental setup, but also to design new molecules (such as drugs and inhibitors), catalysts, and materials with tailored properties. A commonly employed computational strategy to study chemical reactions or conformational changes in molecules is by using total energy calculations and structure optimizations using quantum mechanical or molecular mechanical force fields. Finite temperature effects and zero-point energy corrections are then added posterior by computing quantum mechanical partition functions under the harmonic assumption. Such an approach is straightforward for studying small molecules in gas phase or in continuum solvent. When reactions in condensed matter environment (like reactions in explicit water or other solvents) are studied, the aforementioned strategies cannot give reliable results. This is due to the presence of plethora of conformations of the solute-solvent system in the reactant/product states that have to be accounted for the correct estimation of conformational entropy and free energy. On the other hand, molecular dynamics (MD) techniques can be used to address this problem in an efficient manner. Here, all the relevant conformational states are sampled within a classical trajectory of atoms at a finite temperature.

MD is widely used in studying chemical reactions and conformational changes in soft-matter systems and have been successfully applied to large number of problems across the disciplines in science and technology. Despite of this, MD methods face severe limitation in directly applying it for studying conformational changes and chemical reactions. This drawback originates due to the infrequent transitions between the minima on a potential energy landscape, which are separated with barriers much higher than k_BT, where k_B is the Boltzmann constant and T is the temperature of the system. The time step used in MD simulations is orders of magnitude less than the mean passage time of barrier crossing events. As a result, trajectories are often trapped in a potential energy minimum, while the transition between minima is a "rare event"[1–7].

A number of methods have been proposed to overcome this limitation in MD by accelerating otherwise infrequent transitions; for more details see Refs. 1–7. One of the popular classes of such methods rely on coarse graining the underlying dynamics in collective variable (CV) space. If $\{S(\mathbf{R})_\alpha\}$ is the set of CVs which are functions of nuclear coordinates, then free energy hypersurface in CV space can be computed as

$$F(\mathbf{s}) = -k_B T \ln P(\mathbf{s}) \tag{1}$$

where the probability distribution

$$P(\mathbf{s}) \equiv \left\langle \prod_\alpha \delta(S_\alpha(\mathbf{R}) - s_\alpha) \right\rangle \tag{2}$$

which is calculated by binning the CV values from a canonical ensemble trajectory. In biased sampling methods[2], barrier crossing is accelerated by applying a bias potential $V^b(\mathbf{s})$. In such cases[8],

$$P(\mathbf{s}) = \tilde{P}(\mathbf{s})\, e^{\beta V^b(\mathbf{s})}$$

where $\tilde{P}(\mathbf{s})$ is the historgram of CVs computed as in eq. (2) from a biased trajectory and $\beta = (k_B T)^{-1}$. One of the common methods in this family of methods is the Umbrella Sampling (US)[8,9], where a harmonic bias potential $W_h(s)$ is applied and

$$W_h(s) = \frac{1}{2}\kappa_h \left(s - s_h^0\right)^2, \; h = 1, \cdots, M. \tag{3}$$

Here κ_h, is the curvature of the umbrella potential centered at the CV value s_h^0, and M such umbrella biases are placed at different CV values. The biased distributions $\{P_h^u(\mathbf{s})\}$ are then combined and reweighted using the Weighted Histogram Analysis Method (WHAM)[10,11]. In WHAM, the following equation is self-consistently solved

$$P(s) = \frac{\sum_{h=1}^{M} n_h P_h^u(s)}{\sum_{h=1}^{M} n_h \exp[\beta f_h] \exp[-\beta W_h(s)]} \tag{4}$$

where

$$\exp(-\beta f_h) = \int ds \exp[-\beta W_h(s)] P(s)$$

Here n_h is the number of frames in the trajectory for the h-th umbrella window. The advantage of the US method is that free energy along a specific coordinate or a part of a high dimensional surface can be computed in a controlled fashion. However, the efficiency of the approach decreases with increasing dimensionality of the CV space. Most of the US simulations are done along one CV only. As a result, the convergence of $F(\mathbf{s})$ with respect to simulation time is poor. Several transverse coordinates need to be enhanced sampled to obtain quick and correct convergence of $F(\mathbf{s})$[7].

Metadynamics (MTD)[12,13] is an alternative biased sampling approach for exploring and computing $F(\mathbf{s})$. In MTD, a time dependent bias $V^b(\mathbf{s}, t)$ is applied to the system, which depends on the history of the CVs, $\mathbf{s}(t)$, where

$$V^b(\mathbf{s},t) = \sum_{\tau<t} w(\tau) \exp\left[-\frac{(\mathbf{s}-\mathbf{s}_\tau)^2}{2(\delta s)^2}\right] \tag{5}$$

with

$$w(\tau) = w_0 \exp\left[-\frac{V^b(\mathbf{s},t)}{k_B \Delta T}\right] \tag{6}$$

Here $w(\tau)$ is the height of the Gaussian function at time τ, δs is the parameter determines the width of the Gaussian function, and the ΔT parameter affects the tempering of the Gaussian height as a function of time[14]. For the limit $\Delta T \to \infty$, the Gaussian height $w(\tau) = w_0$, and becomes independent of the bias added at a time τ. Free energy surface $F(\mathbf{s})$ can be computed from the bias potentials directly (without directly computing $P(\mathbf{s})$), given by

$$F(\mathbf{s}) = -\gamma V^b(\mathbf{s}, t \to \infty) + \text{constant} \tag{7}$$

where $\gamma = (T + \Delta T)/\Delta T$. MTD has been successfully applied to various problems in chemistry, biology and material sciences; see reviews[15–22] for more details. MTD explores the CV space $\mathbf{s}$ in a chemically-unbiased manner and the system is driven in a self-guided way. The method is widely employed to sample free energy surface spanned in two or three CVs. In spite of these benefits, there are several limitations in applying MTD for complex problems. These pertain to its inefficiency in sampling broad and unbound free energy basins, uncontrolled sampling, and poor convergence due to insufficient sampling of hidden transverse coordinates.

Temperature Accelerated Molecular Dynamics or driven-Adibatic Free Energy Dynamics (TAMD/d-AFED)[2,23,24] belongs to a different class of methods[25,26], where temperature is used to steer the accelerated sampling. In this method, the Lagrangian of the system is augmented by introducing

an auxiliary subsystem $\{s_\alpha\}$ as

$$\mathcal{L}_{\mathrm{TAMD}}(\mathbf{R}, \dot{\mathbf{R}}, \mathbf{s}, \dot{\mathbf{s}}) = \mathcal{L}_0(\mathbf{R}, \dot{\mathbf{R}}) + \sum_{\alpha=1}^{n} \frac{1}{2}\mu_\alpha \dot{\mathbf{s}}_\alpha^2 - \sum_{\alpha=1}^{n} \frac{k_\alpha}{2}(S_\alpha(\mathbf{R}) - s_\alpha)^2 \quad (8)$$

where $\mathcal{L}_0$ is the original Lagrangian of the system and μ_α is the mass of an extended degrees of freedom. Here, s_α is coupled to the corresponding CV, $S_\alpha(\mathbf{R})$, by a harmonic potential where $\{k_\alpha\}$ is the related coupling constant. Most importantly, **s** variables are kept at a much higher temperature (T_s) than the physical degrees of freedom (T) using separate thermostats for the two subsystems. The parameters k_α, and μ_α are chosen such that the dynamics of the auxiliary degrees of freedom is adiabatically decoupled from the rest in order to prevent any heat flow between the two subsystems. Finally, the free energy surface can be reconstructed from the probability distribution of **s** at high temperature ($\tilde{P}(\mathbf{s})$) as[25,2,23],

$$F(\mathbf{s}) = -k_B T_s \ln \tilde{P}(\mathbf{s}) + \text{constant} \quad (9)$$

where $T_s >> T$. This method has the advantage that bias potentials are not used and the sampling of a high dimensional space is nearly parallel. In MTD, the bias is built along the dynamics of **s** in a serial manner, which becomes increasingly inefficient with the increasing the dimensionality of the space. Thus, TAMD/d-AFED allows one to sample large number of CVs; see the recent review[7]. As $F(\mathbf{s})$ has to be reconstructed directly from probability distribution, accurate computation of $F(\mathbf{s})$ requires converged $\tilde{P}(\mathbf{s})$, which in turn requires multiple recrossings between the basins of our interest. Further, in TAMD/d-AFED, a controlled sampling of CV space (unlike US) is difficult and the efficiency of exploration becomes an issue when the basin is broad and unbound.

To alleviate the problems of these three methods (i.e. US, MTD and TAMD/d-AFED) while making use of their advantages, we have recently proposed a new sampling method called Temperature Accelerated Sliced Sampling (TASS)[27,7]. In this method, we combine these three methods in a specific way. TASS permits one to reconstruct a high dimensional free energy surface in an efficient manner. The method has the flexibility to sample large and different numbers of transverse coordinates along the extent of the reaction. Technical details of this method are discussed in the next section. TASS has been applied to study conformational changes of small peptides[27], chemical reactions in enzymes[28], ligand dissociation in proteins[29], and catalytic reactions in zeolites[30].

In this work, we will first discuss the protocols for the appropriate choice of TASS parameters. Then we apply the method in exploring the five-dimensional free energy surface of alanine tripeptide in explicit water. We chose solvated alanine tripeptide for a detailed study as this is a suitable system to benchmark sampling techniques. We report here the well converged free energy surface of the molecule and carry out detailed analysis.

2. Methods and models

2.1. TASS

In TASS[27,7], we use the extended Lagrangian $\mathcal{L}_{\mathrm{TASS}}$, where

$$\mathcal{L}_{\mathrm{TASS},h}(\mathbf{R}, \dot{\mathbf{R}}, \mathbf{s}, \dot{\mathbf{s}}) = \mathcal{L}_{\mathrm{TAMD}}(\mathbf{R}, \dot{\mathbf{R}}, \mathbf{s}, \dot{\mathbf{s}}) - W_h^b(s_1) - V^b(s_2, t), \; h = 1, \cdots, \mathrm{M}, \quad (10)$$

where $\mathbf{s} = \{s_1, s_2, \ldots, s_n\}$ and $\mathcal{L}_{\mathrm{TAMD}}$ is given by eq. (8). The biases, $W_h^b(s_1)$ and $V^b(s_2, t)$ along the CVs s_1 and s_2 are given by eqs.(3) and (5), respectively. Thus in TASS, all the n CVs are sampled by high temperature as in TAMD, while along s_1 US is carried out and along s_2 one-dimensional MTD sampling is performed. The biased probability distribution is then computed from the histogram of CVs. The unbiased distribution and the free energy hypersurface is then obtained by a series of reweighting and WHAM. First, for every umbrella window, MTD bias potential is reweighted by Tiwary-Parrinello[31] scheme to obtain,

$$\tilde{P}_h^u(\mathbf{s}') = \left\langle \prod_\alpha \delta(s_\alpha - s'_\alpha) \exp\left\{\beta_s \left[V^b(s_2, t) - c(t)\right]\right\} \right\rangle \quad (11)$$

where

$$c(t) = \beta_s^{-1} \ln \left[\frac{\int ds_2 \exp\{\beta_s \gamma_s V^b(s_2, t)\}}{\int ds_2 \exp\{\beta_s (\gamma_s - 1) V^b(s_2, t)\}} \right]$$

with $\beta_s = (k_B T_s)^{-1}$ and $\gamma_s = (T_s + \Delta T)/\Delta T$. As next, the set of probability distributions $\{\tilde{P}_h^u(\mathbf{s})\}$ is combined using WHAM in the usual manner (eq. (4)) to get the distribution $\tilde{P}(\mathbf{s})$. Free energy surface $F(\mathbf{s})$ at temperature T can be obtained from $\tilde{P}(\mathbf{s})$ using eq. (9).

The advantage of TASS is that large number of CVs can be sampled in a parallel manner, similar to TAMD/d-AFED.

Further, a controlled sampling along s_1 is possible because of the US bias. This also aids in quick convergence of free energies compared to conventional TAMD/d-AFED. MTD bias along s_2 permits to overcome free energy barriers in the direction of this transverse coordinate in an efficient manner.

2.2. Collective variables to sample conformations of alanine tripeptide in explicit water

Here we study the free energy landscape of alanine tripeptide in explicit water. Different conformational states (Fig. 1) of alanine tripeptide are expected to be sampled by TASS. These conformational states can be characterized with the Ramachandran-map of the system, and therefore we choose the Ramanchandran-angles, ϕ_1, ϕ_2, ψ_1, and ψ_2 as CVs for enhance sampling. Free energy surface along four CVs is practically difficult to sample by MTD or US.

Choice of CVs are usually done based on chemical intuitions about the chemical reaction of our interest. Ideally, such CVs should be able to distinguish reactants, products and transition state. Since TASS allows large number of CVs, we have the flexibility to use large number of transverse coordinates to accelerate the convergence in free energies and to prevent the system getting trapped in conformational states along the orthogonal directions; see Ref. 7 and references therein.

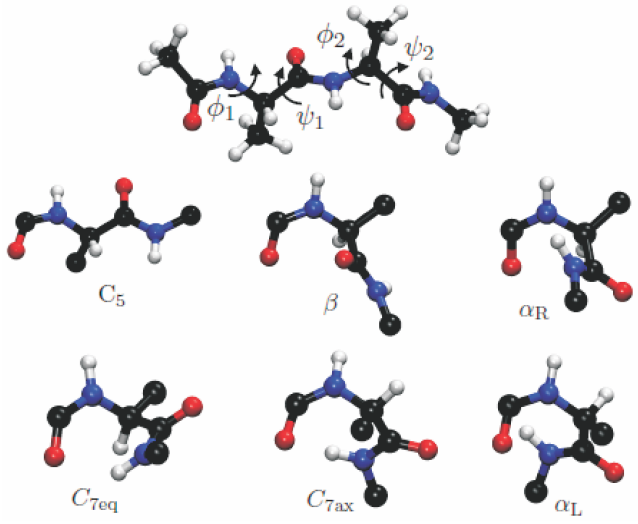

Fig. 1. In the top panel, CVs used for the TASS simualtions are labelled. Different conformational states of alanine tripeptide are shown in the lower panels, where only a part of the peptide is displayed for clarity. Atom colors: O (red), C (black), N (blue), H (white).

US coordinate is mainly chosen along the coordinate which describes the progress of the reaction or along which a controlled sampling is required. For e.g. while studying A+B type reaction, distance between two atoms along which a bond is formed is taken as the US coordinate. MTD bias is applied along any other coordinate that chiefly defines the reaction and large barrier is expected along that CV. All other transverse coordinates, that are vital to enhance the convergence in free energy are sampled by high temperature (as in TAMD/d-AFED).

In the case of alanine tripeptide we are expecting large free energy barriers along ϕ_1 and ϕ_2. Here, the choice of biases along ϕ_1 and ϕ_2 is irrelevant, since both the coordinates have identical behavior by symmetry and free energy basins are bound along these coordinates (due to the intrinsic periodicity of torsions). We arbitrarily chose ϕ_1 for US bias, and ϕ_2 for metadynamics bias. All the four angles are enhanced sampled by high temperature.

2.3. Simulation setup

MD calculations of alanine tripeptide were performed using GROMACS-5.1.4[32] interfaced with PLUMED-2.4[33]. We employed AMBER99 force field[34] for the peptide and water molecules were treated by TIP3P (rigid)[35]. A periodic box of size 34×35×30 Å^3 was taken and it contained 785 water molecules and one tripeptide molecule. The initial structure for the solvated peptide for TASS calculations was obtained after 100 ps of NPT ensemble simulation at 300 K and 1 bar. After 2 ns of equilibration in NVT, TASS simulations were launched independently for each umbrella window. A total of 33 umbrella windows were considered along ϕ_1 from $-\pi$ to π, with an interval of 0.2 radians.

Time step of 1 fs was used for the integration of the equations of motion. Particle Mesh Ewald technique[36] was used for the long-range electrostatics, with a radial cutoff of 10 Å was considered. Non-bonded cutoff of 10 Å was used and the neighbor list was updated every 10 MD steps. Temperature of the physical system was controlled using the stochastic thermostat by Bussi *et al.*[37]. The target temperature of the physical system was 300 K. The coupling constant for the Bussi *et al.*[37] thermostat was taken as 100 fs to maintain the system temperature close to 300 K.

Our test calculations showed that the choice of the k_h = 1.2×10^2 kcal mol^{-1} rad^{-2} ensures good overlap of biased

distributions (see Fig. 2). Moreover, the distributions are centered at the equilibrium position of the umbrella windows.

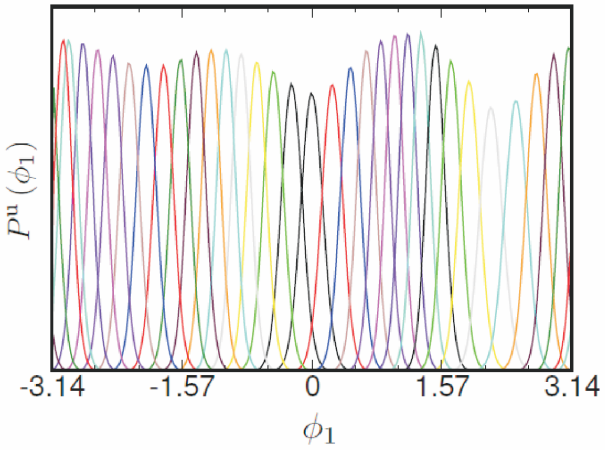

Fig. 2. Biased probability distribution along ϕ_1 (in radians) obtained from US simulations of alanine tripeptide in water. Probability distributions from different umbrella windows are colored differently.

The auxiliary variables were coupled to overdamped Langevin thermostat (as available in PLUMED) with its frictional coefficient set to 0.1 fs^{-1} and target temperature of 900 K. We find that the parameters μ_α = 50 amu $Å^2$ rad^{-2}, κ_α = 1.2×10^3 kcal mol^{-1} rad^{-2} and the time constant corresponding to the thermostat by Bussi *et al.*[37] equals 100 fs were essential to maintain the temperature of the extended and the physical systems close to the corresponding target temperatures during the TASS runs. Further, the physical CVs are oscillating about the slow auxiliary variable, which is ideally required for adiabatic dynamics of the auxiliary variables; see Fig. 3. The well-tempered version of MTD[14] was applied along ϕ_2 with a bias update pace of 500 fs. The initial Gaussian height parameter w_0 = 0.6 kcal mol^{-1}, the width δs = 0.05 radian and ΔT = 900 K were chosen.

For demonstrating the performance of TASS, we performed independent well-tempered MTD and TAMD/d-AFED[23,24] simulations of the system for 10 ns. In the well-tempered simulations, ϕ_1 and ϕ_2 were chosen as the CVs, while the rest of the parameters were the same as in the TASS calculations. In the TAMD/d-AFED simulations, we chose ϕ_1, ψ_1, ϕ_2, and ψ_2 as CVs. The temperature of the auxiliary system, T_s = 900 K was chosen and the frictional

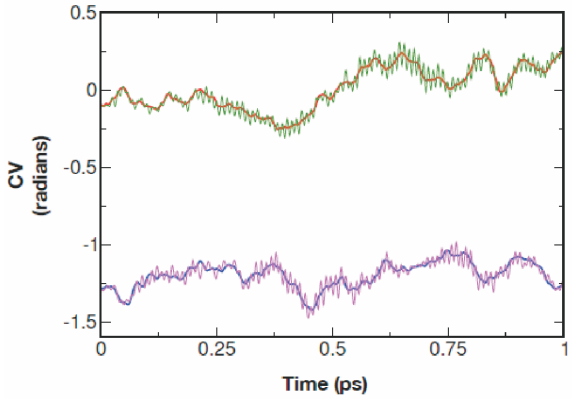

Fig. 3. Plots of ϕ_1 and ϕ_2 (thick blue and red lines) together with the corresponding auxiliary variables (thin green and magenta lines) as the function of time are shown. Here κ_α = 1.2×10^3 kcal mol^{-1} rad^{-2}, μ_α = 50 amu $Å^2$ rad^{-2} were used.

coefficient of the Langevin thermostat connected to the auxiliary system was taken as 0.1 fs^{-1}. All other parameters were the same as in the TASS simulation.

3. Results and discussion

From the TASS trajectories of 10 ns long (per umbrella window), we performed reweighting using eqs. (11), (4), and (9). Convergence of free energy is tested by comparing the free energy surfaces obtained for various simulation lengths. In Fig. 4, projections of $F(\phi_1, \phi_2, \psi_2, \psi_2)$ on to ϕ_1 and ϕ_2 are plotted for 6, 8 and 10 ns long TASS trajectories. Projections to lower dimensions are obtained, for instance along ϕ_1 as,

$$F(\phi_1) = -(\beta_s)^{-1} \ln \left\{ \int d\phi_2 \, d\psi_1 \, d\psi_2 \exp\left[-\beta_s F(\phi_1, \phi_2, \psi_1, \psi_2)\right\} .$$

Clearly, Fig. 4 shows that the free energies are converged to much less than 1 kcal mol^{-1} within 6 ns of the TASS simulation. We would like to particularly mention in passing that

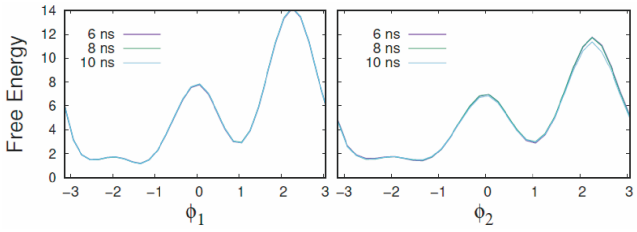

Fig. 4. $F(\phi_1)$ and $F(\phi_2)$ are plotted for different lengths of TASS simulations to demonstrate the convergence with simulation time.

sufficient convergence is achieved even in the domain $\phi \in [1.5,3]$ of high free energies within 6 ns.

Several projections of the free energy surface are shown in Fig. 5. The important conformational states (as in Fig. 1) can be characterized on these free energy landscapes. Our results are in good agreement with the $F(\phi,\psi)$ surface reported for the alanine *dipeptide* in explicit water[38]. Overall, our results agree with the previous report by Tuckerman and co-workers[26]. As expected, the $F(\phi_1, \psi_1)$ and $F(\phi_2, \psi_2)$ surfaces are nearly identical.

The minima **P** and **P′** on the $F(\phi_1, \phi_2)$ (Fig. 5a) correspond to a combination of α_R and β conformations for one of the ALA residue, when the other ALA residue takes the α_L conformation. The minima **Q** corresponds to α_R and β conformations taken by both the ALA residues. Free energy barrier in going from **Q**→**P** is 5 kcal mol^{-1} in explicit water, while it is 3 kcal mol^{-1} higher *in vacuo*. **Q**→**P′** is 1 kcal mol^{-1} higher than **Q**→**P**, both in explicit water and *in vacuo*. Lowering of free energy barriers in solution compared to *in vacuo* was also noticed in the earlier studies[38,26].

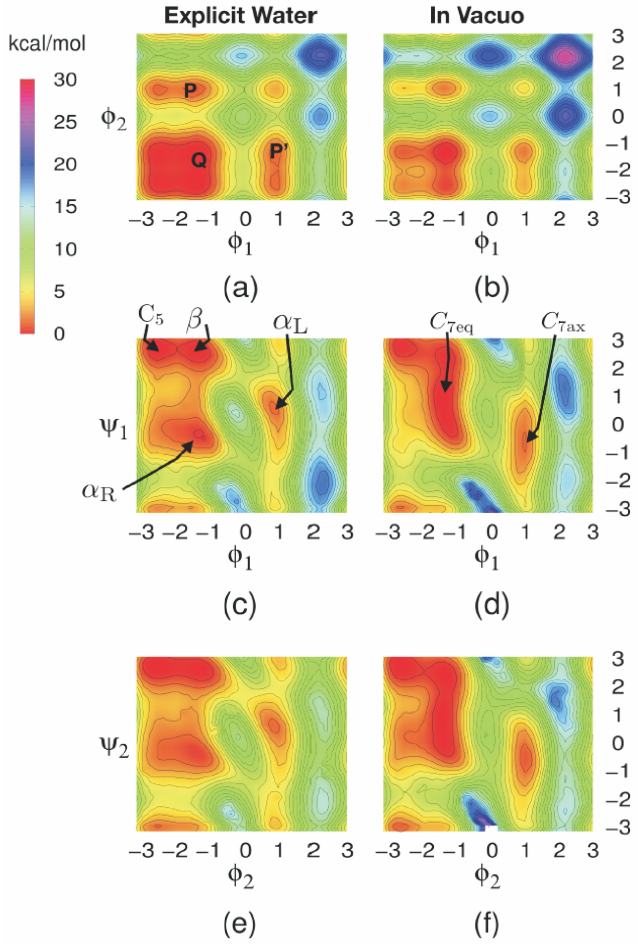

Fig. 5. Several projections of the free energy surface of alanine tripeptide in water are shown in (a), (c), and (e). The same for the peptide *in vacuo* are shown in (b), (d), and (f). The results of alanine tripeptide *in vacuo* are taken from our earlier work[27]. The contours are drawn for every 1 kcal mol^{-1}.

We now compare the efficiency of TASS in exploring the $F(\phi_1, \phi_2, \psi_1, \psi_2,)$ hypersurface, in comparison to well-tempered MTD simulations and TAMD/d-AFED. Free energy surface, Fig. 6a, obtained from the MTD simulations (which sampled ϕ_1 and ϕ_2 as CVs) shows that only a small part of the surface is explored within 10 ns . Moreover, the surface is noisy and not converged. The performance of TAMD/d-AFED seems to be better than MTD in exploring the surface (Fig. 6b). In both these simulations, the domains with high free energies are not well sampled within 10 ns of the simulation. On the other hand, TASS could explore the whole surface within 6 ns. In particular, TASS is able to explore the high free energy regions, thanks to the restraining potentials along ϕ_1. Convergence of free energy slices along ϕ_1 is thereby accelerated due to the restraining potential. It is however noted that the net computational cost of one TASS simulation is M = 33 times higher, as we used 33 independent calculations (corresponding to 33 umbrella restraints). In a parallel computing environment, all the 33 umbrella windows within the TASS calculation can be executed parallel, thereby the overall wall clock computing time for obtaining 10 ns trajectory is the same.

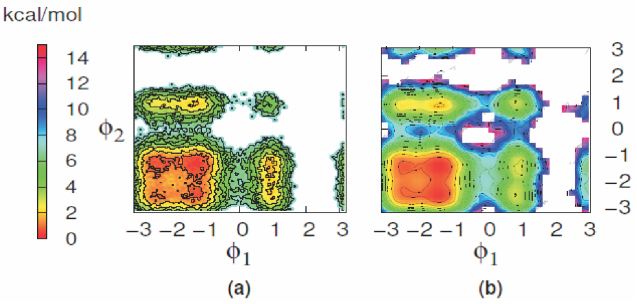

Fig. 6. Free energy surfaces along ϕ_1 and ϕ_2 for alanine tripeptide in explicit water, computed using well-tempered MTD (a), and TAMD/d-AFED (b) from 10 ns simulation are shown. Here, contours are drawn for every 1 kcal mol^{-1}.

4. Conclusions

In this paper, we report the high dimensional free energy surface of alanine tripeptide in explicit water using the TASS technique. Alanine tripeptide is a benchmark system, where the high dimensional space encompassed by the four Ramachandran angle is practically difficult explore fully using the conventional sampling approaches like US and MTD. We demonstrate that, like in the case of alanine tripeptide *in vacuo* reported earlier by us[27], the whole free energy surface can be explored efficiently using TASS. Finally, comparison between the free energy surfaces *in vacuo* and in solution shows some interesting differences, in particular, stable conformations differ and free energy barriers are lowered in the latter case. We hope by reporting the converged free energy surfaces and analyzing the conformational states, this study establishes solvated alanine tripeptide as a benchmark system for methods to explore high dimensional free energy landscapes. The converged high dimensional free energy data will be made available on request.

Acknowledgements

AG and SV thanks Department of Science and Technology, India for their INSPIRE fellowships. ABK is grateful to IIT Kanpur for his PhD fellowship. Authors thank Dr. Shalini Awasthi for valuable inputs. HPC computational facilities at IIT Kanpur and Department of Chemistry are gratefully acknowledged.

Abbreviations

CV, collective variable; d-AFED, driven adiabatic free energy dynamics; MD, molecular dynamics; MTD, metadynamics; TAMD, temperature-accelerated molecular dynamics; TASS, temperature-accelerated sliced sampling; US, umbrella sampling; WHAM, weighted histogram analysis method.

References

1. B. Peters, "Reaction Rate Theory and Rare Events", Amsterdam, Netherlands, Elsevier, 2017.
2. M. E. Tuckerman, "Statistical Mechanics: Theory and Molecular Simulation", 1st ed., Oxford University Press, Oxford, 2010.
3. E. Vanden-Eijnden, *J. Comput. Chem.*, 2009, **30**, 1737.
4. C. D. Christ, A. E. Mark and W. F. van Gunsteren, *J. Comput. Chem.*, 2010, **31**, 1569.
5. S. Bonella, S. Meloni and G. Ciccotti, *Eur. Phys. J. B*, 2012, **85**, 97.
6. O. Valsson, P. Tiwary and M. Parrinello, *Annu. Rev. Phys. Chem.*, 2016, **67**, 159.
7. S. Awasthi and N. N. Nair, "Exploring high-dimensional free energy landscapes of chemical reactions", Wiley Interdisciplinary Reviews, Computational Molecular Science, 9(3), e1398.
8. G. M. Torrie and J. P. Valleau, *Chem. Phys. Lett.*,1974, **28**, 578.
9. J. Kästner, *WIREs Comput. Mol. Sci.* , 2011, **1**, 932.
10. A. M. Ferrenberg and R. H. Swendsen, *Phys. Rev. Lett.*, 1989, **63**, 1195.
11. S. Kumar, J. M. Rosenberg, D. Bouzida, R. H. Swendsen and P. A. Kollman, *J. Comput. Chem.*, 1992, **13**, 1011.
12. A. Laio and M. Parrinello, *Proc. Natl. Acad. Sci. USA*, 2002, **99**, 12562.
13. M. Iannuzzi, A. Laio and M. Parrinello, *Phys. Rev. Lett.*, 2003, **90**, 238302.
14. A. Barducci, G. Bussi and M. Parrinello, *Phys. Rev. Lett.*, 2008, **100**, 020603.
15. A. Laio and M. Parrinello, "Computing free energies and accelerating rare events with metadynamics", Vol. 1, eds. Ferrario M. G. Ciccotti and K. Binder, Springer, Berlin, 2006.
16. B. Ensing, M. D. Vivo, Z. Liu, P. Moore and M. L. Klein, *Acc. Chem. Res.*, 2006, **39**, 73.
17. A. Barducci, M. Bonomi and M. Parrinello, *WIREs Comput. Mol. Sci.*, 2011, **1**, 826.
18. A. Laio and F. L. Gervasio, *Rep. Prog. Phys.*, 2008, **71**, 126601.
19. L. Sutto, S. Marsili and F. L. Gervasio, *Rev. Comput. Mol. Sci.*, 2012, **2**, 771.
20. C. Abrams and G. Bussi, *Entropy*, 2014, **16**, 163.
21. G. Bussi and D. Branduardi, in: 'Free-Energy Calculations with Metadynamics: Theory and Practice', Wiley Blackwell, 2015, pp. 1-49.
22. F. Pietrucci, *Rev. Phys.*, 2017, **2**, 32.
23. L. Maragliano and E. Vanden-Eijnden, *Chem. Phys. Lett.*, 2006, **426**, 168.
24. J. B. Abrams and M. E. Tuckerman, *J. Phys. Chem. B*, 2008, **112**, 15742.
25. L. Rosso, P. Mináry, Z. Zhu and M. E. Tuckerman, *J. Chem. Phys.*, 2002, **116**, 4389.
26. L. Rosso, J. B. Abrams and M. E. Tuckerman, *J. Phys. Chem. B,* 2005, **109**, 4162.
27. S. Awasthi and N. N. Nair, *J. Chem. Phys.*, 2017, **146**, 094108.
28. S. Awasthi, S. Gupta, R. Tripathi and N. N. Nair, *J. Phys. Chem. B*, 2018, **122**, 4299.
29. N. Vithani, P. K. A. Jagtap, S. K. Verma, R. Tripathi, S. Awasthi, N. N. Nair, *et al., Structure*, 2018, **26**, 459.

30. S. K. Sahoo and N. N. Nair, *Front. Chem.*, 2018, **6**, 275.
31. P. Tiwary and M. Parrinello, *J. Phys. Chem. B*, 2014, **119**, 736.
32. H. J. C. Berendsen, D. van der Spoel and R. van Drunen, *Comput. Phys. Commun.*, 1995, **91(1)**, 43.
33. M. Bonomi, D. Branduardi, G. Bussi, C. Camilloni, D. Provasi, P. Raiteri, *et al., Comput. Phys. Commun.*, 2009, **180**, 1961.
34. J. A. Maier, C. Martinez, K. Kasavajhala, L. Wickstrom and K. E. Hauser, *J. Chem. Theory. Comput.*, 2015, **11**, 3696.
35. A. D. MacKerell, D. Bashford, M. Bellott, R. L. Dunbrack, J. D. Evanseck, M. J. Field, *et al., J. Phys. Chem. B*, 1998, **102(18)**, 3586. PMID: 24889800.
36. U. Essmann, L. Perera, M. L. Berkowitz, T. Darden, H. Lee and L. G. Pedersen, *J. Chem. Phys.*, 1995, **103(19)**, 8577.
37. G. Bussi, T. Zykova-Timan and M. Parrinello, *J. Chem. Phys.*, 2009, **130(7)**, 074101.
38. N. Deng, B. Zhang and R. Levy, *J. Chem. Theory. Comput.*, 2015, **11**, 2868.